Eur. Phys. J. B **61**, 427–432 (2008)
DOI: 10.1140/epjb/e2008-00092-2

THE EUROPEAN PHYSICAL JOURNAL B

Correlated electron current and temperature dependence of the conductance of a quantum point contact

C. Sloggett[1], A.I. Milstein[2], and O.P. Sushkov[1,a]

[1] School of Physics, University of New South Wales, Sydney 2052, Australia
[2] Budker Institute of Nuclear Physics, 630090 Novosibirsk, Russia

Received 5 April 2007 / Received in final form 7 August 2007
Published online 5 March 2008 –

Abstract. We investigate finite temperature corrections to the Landauer formula due to electron–electron interaction within the quantum point contact. When the Fermi level is close to the barrier height, the conducting wavefunctions become peaked on the barrier, enhancing the electron–electron interaction. At the same time, away from the contact the interaction is strongly suppressed by screening. To describe electron transport we formulate and solve a kinetic equation for the density matrix of electrons. The correction to the conductance G is negative and strongly enhanced in the region $0.5 \times 2e^2/h \leq G \leq 1.0 \times 2e^2/h$. Our results for conductance agree with the so-called "0.7 structure" observed in experiments.

PACS. 73.23.-b Electronic transport in mesoscopic systems – 72.10.-d Theory of electronic transport; scattering mechanisms – 73.21.Hb Quantum wires – 73.63.Rt Nanoscale contacts

1 Introduction

The conductance of a quantum point contact (QPC) — a 1D constriction in a 2D electron gas — has been known to be quantised in units of $G_0 = 2e^2/h$ since 1988 [1,2]. The observed conductance plateaus can be easily understood in the single-electron picture [3,4].

The "0.7 structure" appears on the lowest conductance step as a narrow extra plateau at $G \approx 0.7$, where we write G, throughout the paper, in units of G_0. The structure was first observed by Thomas et al. in 1996 [5] and has been the subject of numerous experiments since [6–11]. The position of the structure varies from 0.5 to 0.7 depending on the device, and the structure becomes more pronounced as the temperature is increased up to at least ∼4 K, where thermal smearing becomes significant. It is not clear from experiment whether the structure survives at $T = 0$. In a longitudinal magnetic field, which breaks the spin degeneracy, the structure evolves smoothly to the 0.5 plateau that is expected in the single-electron picture.

Observations of the 0.7 structure have created much theoretical interest. There have been suggested explanations based on spontaneous magnetization within the contact [12–17], charge density waves within the contact [18,19], the Kondo effect [20,21], and even on electron−phonon scattering in the contact [22]. The problem has also stimulated the development of general scattering theory in the presence of leads [23,24].

[a] e-mail: sushkov@phys.unsw.edu.au

In the present paper, using perturbation theory, we consider the finite temperature correction to the Landauer formula for the conductance of a QPC. Our results agree with experimental data on the 0.7 structure. Our approach is based on perturbation theory built on scattering states. We will see below that due to electron screening the Coulomb interaction is localised within the QPC, but we do not have a localised electron within the QPC. This is an important difference between our model and those such as the Kondo scenario suggested in references [20,21].

2 Model

Near the center of the QPC the single-particle dynamics are described by the parabolic saddle-point potential

$$U = U_0 - \frac{1}{2}m\omega^2 x^2 + \frac{1}{2}m\omega_y^2 y^2, \qquad (1)$$

see, e.g., reference [4]. Here m is the effective electron mass and U_0 is the electrostatic potential at the centre of the QPC. In experiment, U_0 depends on the gate voltage, and parameters ω_y and ω have typical values of $\omega_y/\omega \sim 3$, $\omega_y \sim 4$ meV. Throughout the paper we set $\hbar = k_B = 1$.

The dynamics in the x-direction are described by different channels corresponding to quantization in the y-direction. The lowest, $n = 0$, channel has longitudinal potential $-\frac{1}{2}m\omega^2 x^2$. The $n = 0$ channel becomes open at $E = E_0 \equiv U_0 + \frac{1}{2}\omega_y$. Since the channel opens

smoothly, this energy corresponds to $G = 0.5$. We define $\epsilon = (E - E_0)/\omega$, so that $G = 0.5$ at $\epsilon = 0$, and the transmission probability is [25]

$$t_\epsilon = \frac{1}{1 + e^{-2\pi\epsilon}}. \tag{2}$$

At $\epsilon = 0$ electrons in higher channels, $n > 0$, cannot (without tunneling) penetrate to $x = 0$ but only to $x_n = \pm\sqrt{\frac{2n\omega_y}{m\omega^2}}$. So outside the barrier, from $x_{2D} \sim 2/\sqrt{m\omega}$, many transverse channels are occupied and hence the electron–electron Coulomb interaction is strongly screened. The interaction is unscreened only the top of the barrier, $x = 0$, where the electron density is low. We will treat this localised interaction, within our model, as a delta function; this is the simplest possible approximation, which as we shall see nevertheless leads to interesting results. We approximate the effective electron–electron interaction in the $n = 0$ channel as

$$\frac{e^2}{\kappa|x_1 - x_2|} \to H_{int} = \omega\pi^2 g_e \delta(\xi_1)\delta(\xi_2), \tag{3}$$

where e is the electron charge, κ is the dielectric constant, and we define $\xi = \sqrt{m\omega}x$, the dimensionless distance. In GaAs, $\kappa \approx 13$, $m \approx 0.07m_e$, and for $\omega \sim 1$ meV the dimensionless coupling constant is about unity,

$$g_e \sim \frac{e^2}{\pi^2\kappa}\sqrt{\frac{m}{\omega}} \sim 1. \tag{4}$$

This model immediately suggests an explanation for the absence of pronounced structures on higher conductance steps. For higher steps there are always lower channels penetrating the QPC. This leads to high electron density in the contact and hence to screening even at $x = 0$.

It has been shown that electron–electron interaction inside a uniform wire does not influence conductance [27]. In our case we have the nonuniform potential $-\frac{1}{2}m\omega^2x^2$, so this result does not apply.

3 Single-particle wave functions

To represent single-particle wave functions in the $n = 0$ channel we consider a 1D wire of length L with a potential barrier in the middle of the wire. The details of the potential shape are unimportant apart from the parabolic top. Wave functions are normalised according to

$$\int_{-L/2}^{L/2} |\psi_k|^2 dx = 1. \tag{5}$$

The length L is of the order of the inelastic mean free path in the leads. Away from the barrier the wave function ψ_k is the standard combination of incident, reflected and transmitted waves

$$\psi_k(x) = \begin{cases} \frac{1}{\sqrt{L}}\left(e^{ikx} + R_\epsilon e^{-ikx}\right) & \xi \ll 0 \\ \frac{1}{\sqrt{L}} T_\epsilon e^{ikx} & \xi \gg 0 \end{cases} \tag{6}$$

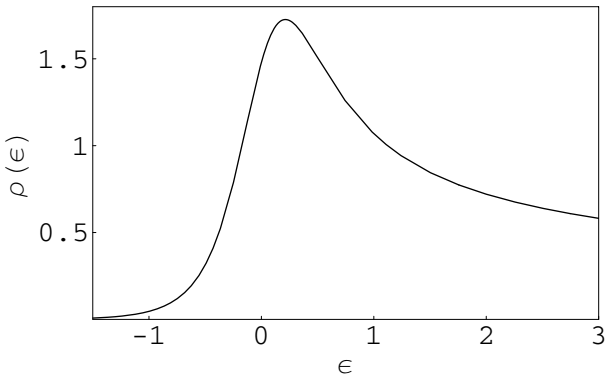

Fig. 1. The probability density at $\xi = 0$ versus the dimensionless energy ϵ.

where R_ϵ and T_ϵ are the complex reflection and transmission coefficients, and the transmission probability is $t_\epsilon = |T_\epsilon|^2$. Near $\xi = 0$ we can consider only the nearby shape of the potential barrier $-\frac{1}{2}m\omega^2x^2 = -\frac{1}{2}\omega\xi^2$, which can be solved to give single-particle wavefunctions of the form (see, e.g., Ref. [25])

$$\psi_k(\xi) \approx \frac{1}{\sqrt{L}}\left(\frac{mv_F^2}{2\omega}\right)^{1/4} \varphi_k(\xi), \tag{7a}$$

$$\varphi_k(\xi) = \sqrt{\frac{e^{\pi\epsilon/2}}{\cosh(\pi\epsilon)}} D_{(i\epsilon-1/2)}(\sqrt{2}\xi e^{-i\pi/4}), \tag{7b}$$

where v_F is the Fermi velocity far from the barrier and D_ν is the parabolic cylinder function. Equations (6) and (7) corresponds to the wave incident from the left, $k \geq 0$. The probability density at the top of the potential given by equation (7b),

$$\rho(\epsilon) = |\varphi_k(0)|^2 = \frac{\pi\exp(\pi\epsilon/2)}{\sqrt{2}\cosh(\pi\epsilon)\,|\Gamma(3/4 - i\epsilon/2)|^2}, \tag{8}$$

is peaked at $\epsilon \approx 0.2$, see Figure 1. This results in enhancement of the interaction (3), and in the end leads to all effects considered in this paper.

We stress that equations (7b) and (8) are given by the exact solution for the parabolic barrier. The normalised equation (7a) assumes a semiclassical approximation at large distances from the top of the barrier where the shape of the barrier is smoothly changing from parabolic to flat.

Note that the peak in Figure 1 is *not* a resonance behaviour such as that seen in the Wolff model [26] or the Kondo or Anderson models, see references [20,21]. These models assume a single particle resonance or a virtual state that give a localised electron. We certainly do not have a localised electron within the QPC and we do not have a resonant/virtual state. This is clear from equation (2): the transmission probability is a smooth function of energy without a resonant behavior. The peak in Figure 1 is due to semiclassical slowing and it is unrelated to a resonance or virtual level.

4 General expression for electron current in terms of the density matrix

The operator of electric current $\hat{j}$ is a single particle operator. In the basis of the scattering states (7) matrix elements $\langle k|\hat{j}|k'\rangle$ are nonzero only if $k' = k$ or $k' = -k$.

$$\langle\psi_k|\hat{j}|\psi_k\rangle = e\frac{k}{m}t_\epsilon, \tag{9}$$

$$\langle\psi_{-k}|\hat{j}|\psi_k\rangle = e\frac{k}{2m}(R^*_\epsilon T_\epsilon - R_\epsilon T^*_\epsilon) = e\frac{k}{m}R^*_\epsilon T_\epsilon. \tag{10}$$

Here we have used the orthogonality condition, $\langle\psi_{-k}|\psi_k\rangle \propto (R^*_\epsilon T_\epsilon + R_\epsilon T^*_\epsilon) = 0$. Therefore the operator $\hat{j}$ can be represented as

$$\hat{j} = \frac{e}{L}\sum_{k,\sigma}\frac{k}{m}\left(t_\epsilon a^\dagger_{k,\sigma}a_{k,\sigma} + R^*_\epsilon T_\epsilon a^\dagger_{-k,\sigma}a_{k,\sigma}\right), \tag{11}$$

where $a^\dagger_{k,\sigma}$ is the creation operator of the electron in state (6), (7) with spin σ. The total electric current is given by the trace of the single particle operator with the density matrix,

$$J = \frac{e}{L}\sum_{k,\sigma}\frac{k}{m}t_\epsilon n_{k,\sigma}. \tag{12}$$

Here $n_{k,\sigma} = \langle\langle a^\dagger_{k,\sigma}a_{k,\sigma}\rangle\rangle$ is the usual occupation number. The double brackets denote quantum and Gibbs averaging. We have used the fact that in the basis of stationary single particle states the offdiagonal matrix element of the density matrix is zero, $\langle\langle a^\dagger_{-k,\sigma}a_{k,\sigma}\rangle\rangle = 0$. This treatment of J is valid with or without electron–electron interaction.

5 Landauer formula for noninteracting electrons

Without electron–electron interaction within the contact the steady state is established due to inelastic collisions in the right and left leads. So, there are two Fermi–Dirac distributions n_{0k} for $k > 0$ and for $k < 0$, with different chemical potentials due to the applied voltage V, so that n_{0k} depends on the direction of current flow, which we write $s = k/|k|$. We write n_{0k} instead of n_k to indicate that this is the noninteracting case. Since the applied voltage V is small one can write

$$n_{0k} = n_f + s\frac{eV}{2\omega}n'_f, \tag{13}$$

where n_f is the equilibrium Fermi–Dirac distribution, $n'_f = -\frac{\partial n_f}{\partial\epsilon} \approx \delta(\epsilon - \mu)$, and μ is the chemical potential in units of ω.

Substitution of (13) into the general equation (12) immediately gives the Landauer formula

$$J = 2\frac{e}{L}\int\frac{Ldk}{2\pi}\frac{k}{m}t_\epsilon n_{0k} = \frac{2e^2}{h}t_\mu V, \tag{14}$$

as expected in the noninteracting case. In units of G_0 this just gives $G = t_\mu$.

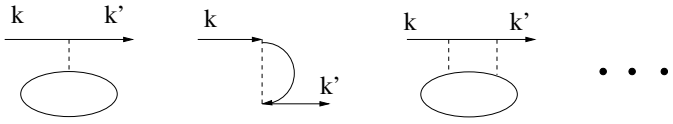

Fig. 2. Corrections to the single particle potential due to electron–electron interaction. The dashed line shows interaction (3).

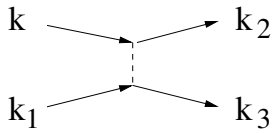

Fig. 3. Four leg diagram describing inelastic scattering.

6 Kinetic equation for occupation numbers with electron–electron interaction

At zero temperature the interaction (3) in the leading order gives the usual elastic direct and exchange diagrams for the single-particle scattering amplitude, see Figure 2. The corresponding corrections renormalise height of the single particle potential, renormalise the frequency ω in the potential and even make the effective potential slightly nonparabolic. Nevertheless this does not materially change the profile of the transmission coefficient (2). We have checked numerically that the same is true to higher orders in perturbation theory. Thus the interaction (3) treated perturbatively does not influence the Landauer formula and does not materially change the shape of the transmission coefficient at zero temperature.

At nonzero temperature, the interaction (3) leads to two different effects. The first is related to two-leg diagrams describing elastic scattering and shown in Figure 2. This effect gives just a weak temperature-dependent renormalisation of the effective potential $-\frac{1}{2}m\omega^2x^2$, similar to the zero-temperature effect discussed above. This does not materially change the profile of the transmission coefficient. The second effect, related to four-leg diagrams describing inelastic scattering, Figure 3, gives a nontrivial correction to conductance. To account for this inelastic scattering we need to discuss equilibration, for which we formulate a kinetic equation.

Let us first consider the case without electron–electron interaction. The scattering states equilibrate to n_{0k} due to collisions in the leads. We can write the kinetic equation

$$\frac{\partial n_k}{\partial t} = -\frac{n_k - n_{0k}}{\tau}, \tag{15}$$

where τ is the relaxation time in the leads. For *any small* deviation from equilibrium, the occupation numbers must obey this equation simply because the equilibrium density matrix is diagonal in the basis of the scattering states [28], and there is no source of equilibration other than the relaxation effect in the leads. This is a nonlocal kinetic equation, as one cannot in principle apply it independently to any particular point within the QPC. The equation describes a region of the size of the inelastic mean free path L

around the contact. This kinetic equation is in principle also valid for finite bias V, but in the present paper we consider only an infinitesimal bias where n_{0k} is given by equation (13).

To take into account electron–electron interaction in the QPC, we consider the basic scattering event of Figure 3. We obtain a collision term in the kinetic equation [29]

$$\frac{\partial n_k}{\partial t} = -\frac{n_k - n_{0k}}{\tau} + \mathrm{St}(n_k), \tag{16}$$

$$\mathrm{St}(n_k) = 2\pi \int \frac{L dk_1}{2\pi}\frac{L dk_2}{2\pi}\frac{L dk_3}{2\pi} |M_{kk_1k_2k_3}|^2 \times [n_{k_2}n_{k_3}(1-n_k)(1-n_{k_1}) - n_k n_{k_1}(1-n_{k_2})(1-n_{k_3})] \times \delta(E_k + E_{k_1} - E_{k_2} - E_{k_3}).$$

Here $M_{kk_1k_2k_3}$ is the matrix element of the interaction (3). This matrix element corresponds to the real transition between quantum states, $|k, k_1\rangle \to |k_2, k_3\rangle$, as shown in Figure 3. Therefore in the matrix element the initial and final wave functions are given by (7). Note that this differs from the Sommerfeld rule, used for the scattering amplitude, where initial wavefunctions are given by equation (7), while final wavefunctions are $\psi_k^{(-)}(x) = \psi_{-k}^*(x)$. (For a description of the Sommerfeld rule, see, e.g., [30].)

7 Conductance with electron–electron interaction

Using occupation numbers from equation (13) and expanding the collision integral of equation (16) up to the first power in the bias V, we find the integral at $T \ll \omega$,

$$\mathrm{St}(n_k) = -\frac{T^2 eV L^3}{12 v_F^3}\delta(E_k - \omega\mu) \times \sum_{s_1 s_2 s_3} [s + s_1 - s_2 - s_3] |M_{kk_1k_2k_3}|^2. \tag{17}$$

All legs in the matrix element are taken at the Fermi surface, so we need only perform summations over the directions s_1, s_2, s_3. Calculating the matrix elements of interaction (3) with the wave functions (7) we find

$$\mathrm{St}(n_k) = -\frac{T^2 eV L^3}{3 v_F^3} s\delta(E_k - \omega\mu) \times \left(|M_{++--}|^2 + |M_{+++-}|^2\right) = -seV\frac{\pi^4 g_e^2}{6}\frac{v_F}{L}\left(\frac{T}{\omega}\right)^2 \rho^4(\mu)\delta(E_k - \omega\mu), \tag{18}$$

where $\rho(\mu)$ is given by (8). Equation (18) leads to the following steady-state solution of the kinetic equation (16)

$$n_k = n_f + \frac{eV}{2} s\delta(E_k - \omega\mu) \times \left\{1 - \frac{\pi^4 g_e^2}{3}\frac{\tau v_F}{L}\left(\frac{T}{\omega}\right)^2 \rho^4(\mu)\right\}. \tag{19}$$

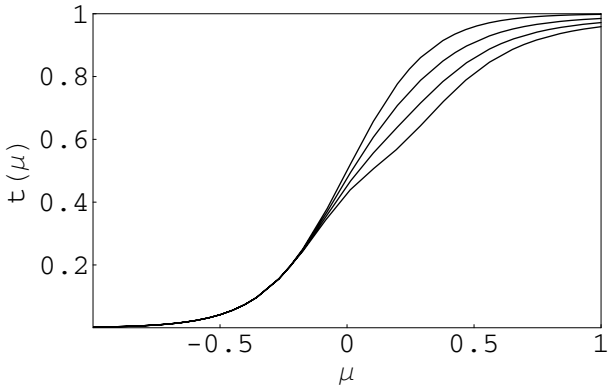

Fig. 4. Conductance in units of $2e^2/h$ versus μ (chemical potential in units of ω) for different temperatures in the weak coupling limit, $g_e \ll 1$. The uppermost curve corresponds to $g_e T = 0$, while the lowest is $g_e T \approx 0.3$ K, assuming $\frac{\tau v_F}{L} \approx 1$.

Substitution of this expression into equation (12) gives an altered transmission probability (or conductance in units of G_0)

$$t_\mu \to \overline{t}_\mu = t_\mu \left\{1 - \frac{\pi^4 g_e^2}{3}\frac{\tau v_F}{L}\left(\frac{T}{\omega}\right)^2 \rho^4(\mu)\right\}. \tag{20}$$

This result is justified only if the second term in brackets is small. The term is due to the current of correlated electrons. It will be most significant within the region $0.5 \times 2e^2/h \le G \le 1.0 \times 2e^2/h$, since above $G = 0.5$ electrons can flow without tunneling, leading to the peak in $\rho(\mu)$. The length L is of the order of the mean free path in the leads, so it is most natural to assume that the factor $\tau v_F/L$ in (20) is of the order of unity, though we cannot exclude some dependence of the factor on temperature. In the latter case the T^2 dependence of the correlated current will be modified.

A set of plots of $\overline{t}_\mu$ for different temperatures is shown in Figure 4. Though the result looks quite sensible it is obtained for $g_e \ll 1$. However, according to our estimate (3), the constant is not small, $g_e \sim 1$, and hence virtual rescattering must be taken into account.

8 Renormalization of the coupling constant due to rescattering

The leading correction to the Born scattering amplitude Figure 3 is given by the diagrams shown in Figure 5. This correction is equivalent to renormalization of the coupling constant, $g_e \to g_e + \delta g_e$, where $\delta g_e(\mu) = 2g_e^2 K(\mu)$ and

$$K(\mu) = \frac{1}{4}\int_{-\infty}^{\infty}\int_{-\infty}^{\infty} \rho(\epsilon_1)\,\rho(\epsilon_2)\left\{\frac{\theta(\epsilon_1 - \mu)\theta(\epsilon_2 - \mu)}{2\mu - \epsilon_1 - \epsilon_2} + \frac{\theta(\mu - \epsilon_1)\theta(\mu - \epsilon_2)}{\epsilon_1 + \epsilon_2 - 2\mu} - 2\,\frac{\theta(\mu - \epsilon_1)\theta(\epsilon_2 - \mu)}{\epsilon_1 - \epsilon_2}\right\} d\epsilon_1\, d\epsilon_2. \tag{21}$$

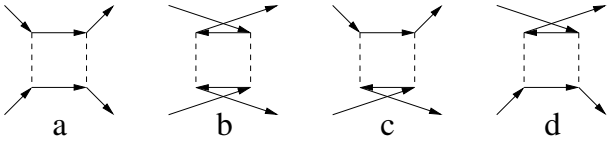

Fig. 5. The leading correction to the matrix element.

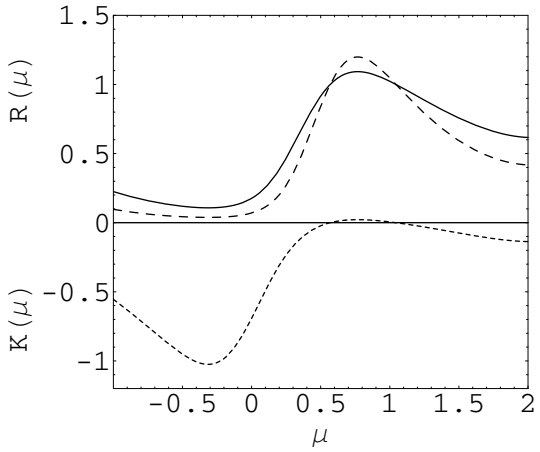

Fig. 6. Dashed line: the function $K(\mu)$ for the second order correction. Solid line: Brueckner correction factor $R(\mu)$ for $g_e = 1$. Long dashed line: Brueckner correction factor $R(\mu)$ for $g_e = 2$.

Here $\theta(y)$ is the step function. The first term in $K(\mu)$ (diagram Fig. 5a) is logarithmically divergent at $\epsilon_1, \epsilon_2 \to +\infty$. The divergence is a result of the contact approximation (3). The point is that the δ-functions in equation (3) in reality should be replaced by bell-shaped functions with width of the order of the barrier size, $\sim 1/\sqrt{m\omega}$, which is also the screening scale. When the electron wavelength λ is larger than this size one can ignore the finite width and use the contact (δ-function) approximation (3). However, when the energy is large, $\epsilon \gg 1$, the electron wave function oscillates within the barrier size, and hence the contact approximation strongly overestimates the Coulomb matrix element. This leads to a logarithmic ultraviolet divergence of (21). To fix the problem, we just introduce an ultraviolet cutoff Λ, $\epsilon_1 + \epsilon_2 \leq \Lambda$. Dependence on the cutoff is weak and we will present all results for $\Lambda = 2$. The integrals in (21) cannot be calculated analytically. However numerical integration is very simple and we present a plot of $K(\mu)$ in Figure 6.

Since the coupling constant $g_e \sim 1$, the second order correction alone is not sufficient. However in this regime the Brueckner approximation [31] usually works well, see analysis in reference [32]. Since the kernel $K(\mu)$ is independent of external momenta, the Brueckner approximation is equivalent to the summation of a geometrical progression, and hence the renormalised coupling constant g_R is

$$g_R^2 = g_e^2 R(\mu), \quad R(\mu) = \frac{1}{[1 - 2g_e K(\mu)]^2}. \qquad (22)$$

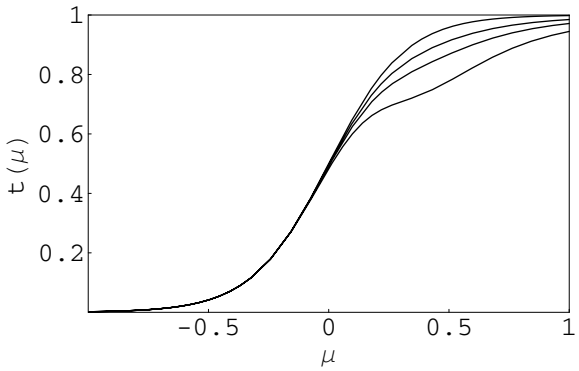

Fig. 7. Conductance in units of $2e^2/h$ versus μ (chemical potential in units of ω) for different temperatures in the intermediate coupling limit, $g_e = 1$. The uppermost curve corresponds to $T = 0$, while the lowest is $T \approx 0.3$ K, assuming $\frac{\tau v_F}{L} \approx 1$.

Plots of $R(\mu)$ for $g_e = 1$ and $g_e = 2$ are presented in Figure 6. Figure 7 shows a set of plots of conductance $\overline{t_\mu}$ for different temperatures, using equation (20) with $g_e \to g_R(g_e)$ for $g_e = 1$. The results presented in Figures 4, 7 are very similar to the experimental data on the 0.7 structure. According to our calculation the exact position of the structure depends on the coupling constant g_e: for small g_e it is more like a "0.5 structure" and for $g_e \sim 1$ it is a "0.6–0.7 structure".

9 Longitudinal magnetic field

The effects we have discussed are due to the interaction between electrons with opposite spins. The interaction between electrons with parallel spins vanishes because the exchange diagram exactly cancels out the direct one for the contact Hamiltonian (3). Therefore under an applied longitudinal magnetic field B we should take $\rho^4(\mu) \to \rho^2(\mu)\rho^2(\mu')$. Here $\mu' = \mu - (2g_s\mu_B)B/\omega$, where g_s is the gyromagnetic ratio and μ_B is the Bohr magneton. Since $\rho(\mu)$ is a peaked function (Fig. 1) a magnetic field $B \sim \omega/(2g_s\mu_B) \sim 10$ T effectively switches off the interaction. At the same time, the ordinary spin-splitting of the steps is being switched on. This gives an explanation for the smooth evolution of the 0.7 structure to the 0.5 plateau of non-interacting electrons under a magnetic field. The calculated dependence on magnetic field for $g_e = 1$ and $T = 0.3$ K shown in Figure 8 agrees with experimental data [5] remarkably well.

10 Conclusion

Within perturbation theory, we have considered transport of correlated electrons through a quantum point contact. At zero temperature, the approach results in the usual Landauer formula and the conductance does not show any structures. However at nonzero temperature the electron–electron interaction gives rise to a current of correlated electrons which scales as temperature squared at very low temperatures. The corresponding correction to conductance is negative and strongly enhanced in the region

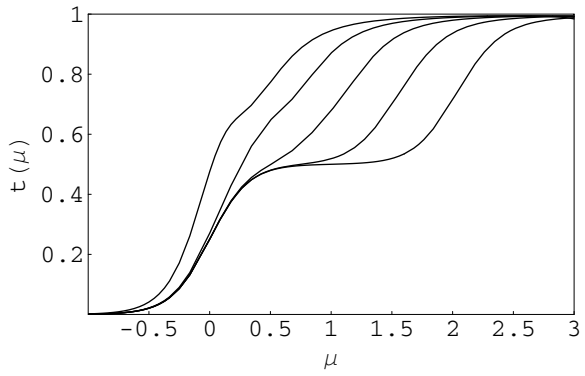

Fig. 8. Conductance in units of $2e^2/h$ versus μ (chemical potential in units of ω) for $g_e = 1$, $T = 0.3$ K and different values of longitudinal magnetic field, $2g_s\mu_B B/\omega = 0, 0.5, 1, 1.5, 2$. The uppermost curve corresponds to $B = 0$, while the lowest is $B \approx 17$ T, assuming $\omega = 1$ meV and $g_s = 1$, see reference [5].

$0.5 \times 2e^2/h \leq G \leq 1.0 \times 2e^2/h$, as seen in Figures 4 and 7. We believe that these results are directly relevant to the 0.7 conductance structure. Our model is consistent with the experimental behavior of the 0.7 structure under a magnetic field: a field smoothly "switches off" the effective interaction between electrons, Figure 8. Effects considered in the present paper have a very simple physical origin: the electron wave function at the barrier and hence the electron–electron interaction is strongly peaked when the transmission coefficient is slightly higher than 0.5.

We are grateful to A. Hamilton, Y. Imry, R. Newbury and M. Pepper for helpful comments and discussion. A. I. M. gratefully acknowledges the School of Physics at the University of New South Wales for warm hospitality and financial support during his visit. This work was supported in part by the Australian Research Council.

References

1. D.A. Wharam et al., J. Phys. C **21**, L209 (1988)
2. B.J. van Wees et al., Phys. Rev. Lett. **60**, 848 (1988)
3. R. Landauer, Phys. Lett. A **85**, 91 (1981)
4. M. Büttiker, Phys. Rev. B **41**, 7906 (1990)
5. K.J. Thomas et al., Phys. Rev. Lett. **77**, 135 (1996)
6. K.J. Thomas et al., Phys. Rev. B **58**, 4846 (1998)
7. A. Kristensen et al., Phys. Rev. B **62**, 10950 (2000)
8. D.J. Reilly et al., Phys. Rev. B **63**, 121311 (2001)
9. S.M. Cronenwett et al., Phys. Rev. Lett. **88**, 226805 (2002)
10. P. Roche et al., Phys. Rev. Lett. **93**, 116602 (2004)
11. R. Danneau et al., Appl. Phys. Lett. **88**, 012107 (2006)
12. Chuan-Kui Wang, K.-F. Berggren, Phys. Rev. B **54**, 14257 (1996); Chuan-Kui Wang, K.-F. Berggren, Phys. Rev. B **57**, 4552 (1998)
13. L. Calmels, A. Gold, Solid State Commun. **106**, 139 (1998)
14. N. Zabala, M.J. Puska, R.M. Nieminen, Phys. Rev. Lett. **80**, 3336 (1998)
15. H. Bruus, V.V. Cherepanov, K. Flensberg, Physica E **10**, 97 (2001)
16. A.A. Starikov, I.I. Yakimenko, K.-F. Berggren, Phys. Rev. B **67**, 235319 (2003)
17. D.J. Reilly, Phys. Rev. B **72**, 033309 (2005)
18. B. Spivak, F. Zhou, Phys. Rev. B **61**, 16730 (2000)
19. O.P. Sushkov, Phys. Rev. B **64**, 155319 (2001); **67**, 195318 (2003)
20. Y. Meir, K. Hirose, N.S. Wingreen, Phys. Rev. Lett. **89**, 196802 (2002); K. Hirose, Y. Meir, N.S. Wingreen, Phys. Rev. Lett. **90**, 026804 (2003)
21. P.S. Cornaglia, C.A. Balseiro, Europhys. Lett., **67**, 634 (2004)
22. G. Seelig, K.A. Matveev, Phys. Rev. Lett. **90**, 176804 (2003)
23. R.A. Molina et al., Phys. Rev. B **67**, 235306 (2003)
24. V. Meden, U. Schollwoeck, Phys. Rev. B **67**, 193303 (2003)
25. A. Bohr, B. Mottelson, *Nuclear Structure* (World Scientific, Singapore, 1998), Vol. 2, pp. 372–375
26. P.A. Wolff, Phys. Rev. **15**, 1030 (1961)
27. D. Maslov, M. Stone, Phys. Rev. B **52**, R5539 (1995)
28. M. Büttiker, Phys. Rev. Lett. **65**, 2901 (1990)
29. E.M. Lifshitz, L P. Pitaevskii, *Physical Kinetics* (Pergamon Press, Oxford, New York, 1981)
30. L.D. Landau, E.M. Lifshitz, *Quantum Mechanics* (Pergamon Press, Oxford, New York, 1965)
31. K.A. Brueckner, C.A. Levinson, Phys. Rev. **97**, 1344 (1955)
32. V.A. Dzuba, V.V. Flambaum, O.P. Sushkov, Phys. Lett. A **140**, 493 (1989); V.A. Dzuba, V.V. Flambaum, O.P. Sushkov, Phys. Lett. A **141**, 147 (1989)